IL-4 Receptor Alpha Signaling through Macrophages Differentially Regulates Liver Fibrosis Progression and Reversal

EBioMedicine 29 (2018) 92–103

Contents lists available at ScienceDirect

EBioMedicine

journal homepage: www.ebiomedicine.com

Research Paper

IL-4 Receptor Alpha Signaling through Macrophages Differentially Regulates Liver Fibrosis Progression and Reversal

Shih-Yen Weng [a,b], Xiaoyu Wang [a,b], Santosh Vijayan [a,b], Yilang Tang [b,c], Yong Ook Kim [a,b], Kornelius Padberg [a,b], Tommy Regen [b,c], Olena Molokanova [a,b], Tao Chen [a,b], Tobias Bopp [b,d], Hansjörg Schild [b,d], Frank Brombacher [e], Jeff R. Crosby [f], Michael L. McCaleb [f], Ari Waisman [b,c], Ernesto Bockamp [a,b], Detlef Schuppan [a,b,g,*]

[a] Institute of Translational Immunology, University Medical Center, Johannes Gutenberg University, Mainz, Germany
[b] Research Center for Immunotherapy (FZI), University Medical Center, Johannes Gutenberg University, Mainz, Germany
[c] Institute for Molecular Medicine, University Medical Center, Johannes Gutenberg University, Mainz, Germany
[d] Institute for Immunology, University Medical Center, Johannes Gutenberg University, Mainz, Germany
[e] International Center for Genetic Engineering and Biotechnology, Institute of Infectious Disease and Molecular Medicine, South African Medical Research Council, Cape Town, South Africa
[f] Ionis Pharmaceuticals, Carlsbad, CA, United States
[g] Division of Gastroenterology, Beth Israel Deaconess Medical Center, Harvard Medical School, Boston, MA, United States

ARTICLE INFO

Article history:
Received 29 August 2017
Received in revised form 22 January 2018
Accepted 23 January 2018
Available online 17 February 2018

Keywords:
Fibrosis
IL-4 receptor alpha
Liver
Macrophage
MMP12
Progression
Reversal

ABSTRACT

Chronic hepatitis leads to liver fibrosis and cirrhosis. Cirrhosis is a major cause of worldwide morbidity and mortality. Macrophages play a key role in fibrosis progression and reversal. However, the signals that determine fibrogenic vs fibrolytic macrophage function remain ill defined. We studied the role of interleukin-4 receptor α (IL-4Rα), a potential central switch of macrophage polarization, in liver fibrosis progression and reversal. We demonstrate that inflammatory monocyte infiltration and liver fibrogenesis were suppressed in general IL-4Rα$^{-/-}$ as well as in macrophage-specific IL-4Rα$^{-/-}$ (IL-4Rα$^{\Delta LysM}$) mice. However, with deletion of IL-4Rα$^{\Delta LysM}$ spontaneous fibrosis reversal was retarded. Results were replicated by pharmacological intervention using IL-4Rα-specific antisense oligonucleotides. Retarded resolution was linked to the loss of M2-type resident macrophages, which secreted MMP-12 through IL-4 and IL-13-mediated phospho-STAT6 activation. We conclude that IL-4Rα signaling regulates macrophage functional polarization in a context-dependent manner. Pharmacological targeting of macrophage polarization therefore requires disease stage-specific treatment strategies.
Research in Context: Alternative (M2-type) macrophage activation through IL-4Rα promotes liver inflammation and fibrosis progression but speeds up fibrosis reversal. This demonstrates context dependent, opposing roles of M2-type macrophages. During reversal IL-4Rα induces fibrolytic MMPs, especially MMP-12, through STAT6. Liver-specific antisense oligonucleotides efficiently block IL-4Rα expression and attenuate fibrosis progression.

1. Introduction

Chronic liver diseases can progress to cirrhosis, which is characterized by excessive accumulation of scar tissue (extracellular matrix, ECM) that is mainly composed of fibrillar collagens, glycoproteins and proteoglycans and that leads to severe distortion of the liver vascular architecture (Schuppan and Afdhal, 2008). While activated myofibroblasts and hepatic stellate cells (HSC) are the major producers of the fibrotic scar, their fibrogenic activation and proliferation depends on a complex interplay with other resident or recruited cells and their secreted factors. Here, immune cells, which promote or attenuate fibrogenesis, have become targets of antifibrotic treatments (Friedman et al., 2013; Schuppan and Kim, 2013; Trautwein et al., 2015). Importantly, recent studies of highly

Abbreviations: Arg1, Arginase 1; α-SMA, alpha–smooth muscle actin; ASO, antisense oligonucleotide; BW, body weight; CCL2, chemokine (C-C motif) ligand 2; CCl_4, carbon tetrachloride; Col1a1, procollagen α1(I) transcript; DAPI, 4,6-diamidino-2-phenylindole; DKO, double knockout; ECM, extracellular matrix; Gapdh, glyceraldehyde 3-phosphate dehydrogenase; HSC, hepatic stellate cell; Hyp, hydroxyproline; IFNγ, interferon-gamma; IL-4Rα, interleukin-4 receptor alpha; iNOS, inducible nitric oxide synthase; MMP, matrix metalloproteinase; MRC1, mannose receptor C type 1 (CD206); PDGF, platelet-derived growth factor beta; qPCR, quantitative polymerase chain reaction; SEM, standard error of the mean; STAT3/STAT6, signal transducer and activator of transcription 3 or 6; TGFβ1, transforming growth factor beta 1 transcript; TIMP, tissue inhibitor of metalloproteinase 1; TNF-α, tumor necrosis factor alpha; WT, wildtype.

* Corresponding author at: Institute of Translational Immunology, Research Center for Immune Therapy, University Medical Center, Johannes Gutenberg University, Langenbeckstraße 1, 55131 Mainz, Germany.
E-mail address: detlef.schuppan@unimedizin-mainz.de (D. Schuppan).

https://doi.org/10.1016/j.ebiom.2018.01.028

effective antiviral therapies in hepatitis B or C patients proved cirrhosis to be a reversible condition, but the detailed mechanism underlying reversal remain unclear (Chang et al., 2010; D'Ambrosio et al., 2012; Marcellin et al., 2013).

As precursors of macrophages and dendritic cells, blood monocytes are recruited to sites of injury by cytokines such as CCL2, CCL3 and CCL6, which are abundant in patients with chronic liver diseases and cirrhosis (Karlmark et al., 2009; Marra et al., 1998; Shimizu et al., 2001). In advanced CCl_4-induced liver fibrosis, there is a massive recruitment of CCL2/CCR2-guided monocytes that develop into $CD11b^+$ $F4/80^+$ $Ly\text{-}6C^{hi}$ monocytic macrophages (Karlmark et al., 2009). These infiltrating cells produce cytokines and chemokines with potent pro-inflammatory or direct fibrogenic effects on HSC and (myo)fibroblasts, such as IL-1β, CCL2, CCL5, CCL7, CCL8, CXCL4, TNFα, TGFβ-1, and PDGF-BB (Barron and Wynn, 2011; Mehal and Schuppan, 2015; Ramachandran et al., 2012). With cessation of the damaging stimulus and by yet ill-defined mechanisms, these cells can undergo a shift towards an anti-inflammatory and fibrolytic resident macrophage phenotype.

Resident macrophages may originate from $Ly\text{-}6C^-$ $CCR2^-$ monocytes and have the potential to transform into classically (M1) or alternatively (M2) polarized macrophages in vivo (Egawa et al., 2013). M1- and M2-type polarizations can be induced in vitro by cytokines that also favor T helper (Th)1 vs Th2 cell polarization, i.e., by IFNγ and IL-12 vs IL-4 and IL-13, respectively (Jaguin et al., 2013). M1-type macrophages are considered pro-inflammatory and potentially antifibrotic, while the role of M2-type macrophages, which can be subdivided into at least 5 subtypes, in inflammation and fibrosis is less well defined (Gundra et al., 2017). The various M2-subtypes may exhibit either pro- or anti-fibrotic activity (Borthwick et al., 2016; Gordon and Martinez, 2010; Murray et al., 2014; Sica et al., 2014). This and other observations suggest that the overall functional relevance of the classical M1 and M2 paradigm is limited (Murray et al., 2014). Therefore, also the utility of therapeutic approaches using classical Th1/M1 vs Th2/M2 polarizing cytokines (Barron and Wynn, 2011; Duffield et al., 2013) remains unclear.

IL-4Rα that responds to both IL-4 and IL-13 should represent a central switch for M1- towards M2-type macrophage polarization. Since its cell specific function in inflammation and fibrosis has not been clearly investigated, we extensively characterized its role during liver fibrosis progression and regression, including its myeloid cell-specific deletion and therapeutic inhibition. We show that macrophage IL-4Rα regulates fibrosis progression and reversal discordantly through modulation of macrophage subsets, indicating that antifibrotic therapies targeting IL-4Rα require disease stage-specific pharmacological intervention.

2. Materials and Methods

2.1. Mice

Il4ra$^{-/-}$, *Il4*/*Il13* double knockout (DKO), *Il4ra*$^{fl/fl}$ and $LysM^{Cre}$ mice were on a Balb/c background (Herbert et al., 2004; McKenzie et al., 1999; Mohrs et al., 1999). Balb/c wild type mice were obtained from Janvier (Saint Berthevin Cedex, France). For the generation of *Il4ra*$^{\Delta CD4}$ mice ($CD4^{Cre}$*Il4ra*$^{flox/flox}$) with T cell-specific deletion of IL-4Rα, $CD4^{Cre}$ mice were mated with *Il4ra*$^{flox/flox}$ mice. To generate *Il4ra*$^{\Delta LysM}$ mice ($LysM^{Cre}$*Il4ra*$^{flox/-}$) with myeloid-specific deletion of IL-4Rα, $LysM^{Cre}$*Il4ra*$^{-/-}$, mice were bred with *Il4ra*$^{flox/flox}$ mice. Littermates of $LysM^{Cre}$*Il4ra*$^{flox/-}$ and *Il4ra*$^{flox/-}$ were used as controls in all related studies. All mice were housed under specific pathogen-free conditions. All experiments were performed with female 8- to 16-week-old mice and approved by the ethical committee of the Government of Rhineland Palatinate under the reference number 2317707/G12–1-007.

2.2. Fibrosis Models

Escalating CCl_4 doses (0.875 mL/kg; week 1–3, 1.75 mL/kg; week 4–6, 2.5 mL/kg) were given via oral gavage three times per week during 6 weeks as described (Popov et al., 2011), to induce a primarily parenchymal liver fibrosis. Fibrosis reversal was examined at 1, 2 or 4 weeks after the last CCl_4 treatment. For therapeutic intervention a 3 week CCl_4-regimen was chosen. Diet-induced liver fibrosis, resembling human nonalcoholic steatohepatitis, was induced in 8-week old male mice that were fed a methionine and choline deficient (MCD) diet for 8 weeks. Mice on a methionine and choline sufficient diet (MCS) served as controls (Wang et al., 2018).

2.3. In Vivo and In Vitro Application of Antisense Oligonucleotides (ASOs)

All 2nd-generation chimeric antisense nucleotides (ASOs) were produced by Ionis pharmaceuticals (Calsbad, CA) with base modifications as described (Seth et al., 2008). To enhance binding affinity and avoid degradation by nucleases, the phosphorothioate backbone nucleotides were synthesized with 2-O-methoxyethyl (MOE) or locked 2-O, 4-C-((*S*)-ethylidene) (cEt) modifications in the ribose backbone (3–5 bases at both ends), while the internal 10 nucleotides remained unchanged. ASOs were administered 3 times per week (40 mg/kg in a volume of 10 μL PBS per g BW) by intraperitoneal injection. In short-term progression experiments (CCl_4 for 3 weeks) mice were treated with ASOs during the 3 weeks. Alternatively, ASO treatment was started off CCl_4 for one week to assess efficacy during fibrosis regression. ASO sequences were as follows: Control ASO (Ionis 141923): 5′-CCTTCCCTGAAGGTTCCTCC-3′; IL-4Rα ASO1 (Ionis 629123): 5′-AGTAG GTAGGACAACA-3′; IL-4Rα ASO2 (Ionis 231894): 5′-CCGCTGTTC TCAGGTGACAT-3′; STAT6 ASO: (Ionis 195428), 5′-CCACAGAGACATG ATCTGGG-3′.

2.4. Hydroxyproline (Hyp) Determination

300 mg liver tissue (150 mg from the right and 150 mg from the left liver lobe) was lysed in 5 mL HCl (6 N) at 110 °C for 16 h as previously described(Popov et al., 2005). Briefly, the 5 μL of hydrogenated sediment and Hyp standards (5 points of serial dilutions) were incubated with 50 μL citrate acetate buffer (5% citric acid, 7.24% sodium acetate, 3.4% NaOH and 1.2% glacial acetic acid, pH 6.0) and 100 μL of chloramine-T solution (14.1 mg/mL chloramine T hydrate, 10% n-propanol, 80% citrate acetate buffer) for 30 min at room temperature. Then 100 μL of Ehrlich's reagent (0.17 g/mL 4-dimethylaminobenzaldehyde dissolved in 20.7% perchloric acid and 70.5% n-propanol) were added to the mixture and incubated at 65 °C for 30 min. The reactants were measured for absorbance at 550 nm. Hyp concentrations in liver tissue were determined by their absorbance relative to the standards after subtraction of the reaction after and before Ehrlich's reagent incubation.

2.5. Quantitative PCR

Liver samples (100 mg; 50 mg from the right and 50 mg from the left liver lobe) were lysed in Trizol (Invitrogen, Carlsbad, CA) and 500 ng total RNA was used for reverse transcription (Quanta Bio, Gaithersburg, MD). cDNAs were subjected to qPCR using either the Taqman or SYBR green technology (Applied Biosystems, Foster City, CA) and run on a StepOnePlus real-time PCR system (Applied Biosystems, Foster City, CA). Gene expression was normalized to expression of *Gapdh*. Primers and probes are specified in the Supplemental Information.

2.6. Histology and Immunohistochemistry

Liver tissue was fixed in 4% Roth-Histofix (Carl Roth, Karlsruhe, Germany), dehydrated, embedded in paraffin, sectioned and rehydrated as described (Popov et al., 2005). For Sirius Red staining, rehydrated sections were exposed to 0.1% Direct Red (Sigma-Aldrich, St Louis, MO) in saturated picric acid for 30 min. Slides were examined under the microscope using a 100× magnification and in each case 10 random fields

were analyzed using the ImageJ software package (National Institute of Health, Bethesda, MD).

For immunohistochemistry, rehydrated sections were boiled in 10 mM sodium citrate buffer for 10 min. Endogenous peroxidase was quenched using 3% H_2O_2 in PBS and sections were blocked with 5% goat or horse serum for 1 h, incubated for 1 h with the primary antibody at 4 °C and finally exposed to either a biotinylated or a fluorochrome-conjugated secondary antibody for 1 h at room temperature. The biotin signal was amplified with the VECTASTAIN ABC kit (Vector Laboratories, Burlingame, CA). Sections were developed with diamino-benzidine, counterstained with Hematoxylin and mounted (Roti-Histokitt II, Carl Roth, Karlsruhe, Germany). Fluorescent sections were treated with DAPI (Sigma-Aldrich, St Louis, MO) and mounted using Fluoroshield (Sigma-Aldrich, MO). Primary antibodies were directed to α-SMA (Abcam, Cambridge, UK), Ym1 (Stemcell Technologies, Vancouver, Canada), CD68 (Biorad, Hercules, CA), CD206 (Biolegend, San Diego, CA) and Ly-6G (BD Bioscience, San Jose, CA). Secondary antibodies were either biotinylated goat anti-rabbit IgG (Vector Laboratories, Burlingame, CA) or Alexa Fluor 488 donkey anti-goat antibodies (Invitrogen, Carlsbad, CA).

2.7. Isolation of Hepatic Non-parenchymal Cells

Livers were minced and cells treated with collagenase buffer (0.4% collagenase type IV, Sigma-Aldrich, St Louis, MO), 154 mM NaCl, 5.6 mM KCl, 5.5 mM glucose, 20.1 mM HEPES, 25 mM $NaHCO_3$, 2 mM $CaCl_2$, 2 mM $MgCl_2$, 1.6 nM DNase I (Applichem, Darmstadt, Germany) (pH 7.4) and dispersed with a gentleMACS dissociator (Miltenyi Biotec, Bergisch-Gladbach, Germany). Homogenates were incubated at 37 °C for 30 min, passed through a 100 μm cell strainer (BD Bioscience, San Jose, CA) and centrifuged at 21 ×*g* for 4 min in ice cold PEB buffer (PBS, 2 mM EDTA, 0.5% BSA). Supernatants were centrifuged at 300 ×*g* for 10 min and cell pellets were resuspended in PEB buffer. Red blood cells were lysed by adding 10 volumes of 150 mM NH_4Cl, 10 mM $KHCO_3$, 1 mM EDTA·2Na. Non-lysed immune cells were washed twice and suspended in PEB buffer.

2.8. Isolation of Splenic CD4 T Cells

Spleens were harvested, passed through a 70 μm cell strainer (BD Bioscience, San Jose, CA) and centrifuged at 300 ×*g* for 10 min in ice cold PEB buffer. Pellets were resuspended in PEB and incubated with CD4 microbeads at 4 °C for 15 min. Labelled cells were washed, centrifuged, resuspended in PEB and separated using MACS columns (Miltenyi Biotec, Bergisch-Gladbach, Germany).

2.9. Flow Cytometry

Non-parenchymal liver cells were blocked with the 2.4G2 anti-Fc receptor antibody (BD Bioscience, San Jose, CA) followed by staining with antibodies recognizing CD4, CD8, CD11b, CD11c, CD19, CD45, CD86, CD90.2, F4/80, IL-4Rα, Ly-6C, Ly-6G, MHCII (BD Bioscience, San Jose, CA; Biolegend, San Diego, CA; eBioscience, San Diego, CA). For intracellular staining, cells were fixed in Fix/Perm buffer (BD Bioscience, San Jose, CA), washed in PBS containing 2% serum and incubated in Perm/Wash buffer (BD Bioscience, San Jose, CA) with an anti-CD206 antibody serving as M2 macrophage marker (eBioscience, San Diego, CA). For intracellular detection of IL-4 and IL-13, cells were stimulated with phorbol myristate acetate (PMA, 50 ng/mL), ionomycin (500 ng/mL) and brefeldin (1 μg/mL) at 37 °C for 3 h, fixed, permeabilized as above and subsequently stained with IL-4 and IL-13 antibodies (eBioscience, San Diego, CA). For the determination of phospho-STAT6 or phospho-STAT3, cells were either stimulated with IL-4 (20 ng/mL), IL-13 (20 ng/mL) or IL-6 (100 ng/mL) at 37 °C for 30 min, fixed in 2% formaldehyde for 10 min and permeabilized with cold methanol. After permeabilization, cells were stained with anti-phospho-STAT6 or -STAT3 (BD Bioscience, San Jose, CA). Cell acquisition was performed on a FACS Canto II (BD Bioscience, San Jose, CA) and analyzed with the FLOWJO software (TreeStar, Ashland, OR). Gating Strategy is demonstrated in Fig. S2. Detailed information on all antibodies is listed in Supplemental Information.

2.10. Cell Culture and Transfection

RAW264.7 murine macrophages (ATCC TIB-71) were seeded in 12-well plates (10^5 per well). After 6 h, cells were transfected with IL-4Rα-specific or control ASOs using the jetPEI-Macrophage DNA transfection reagent (Polyplus, Illkirch, France). Sixteen hours after transfection, cells were harvested, lysed in Trizol (Invitrogen, Carlsbad, CA) and subjected to qPCR analysis. For the isolation of peritoneal macrophages, mice were euthanized and i.p. injected with 10 mL DMEM/F12 medium. After a short soft massage of the abdominal area, a small incision was made to recover the injected medium. Cells were isolated by centrifugation and plated in DMEM medium (supplemented with 10% (v/v) fetal bovine serum, 10 mM L-glutamine, 100 IU/mL penicillin, and 100 μg/mL streptomycin). Nonadherent cells were removed 24 h later, and cells were used for further experiments. For the isolation of bone marrow-derived macrophages, mice were euthanized, and femurs and tibias removed. A small cut was made on both ends of the bones, and a 25-G needle attached to a syringe was inserted into the cavity to flush out the bone marrow. The bone marrow cells were centrifugated and then plated in differentiation RPMI-1640 medium (supplemented with 10% (v/v) fetal bovine serum, 10 mM L-glutamine, 100 IU/mL penicillin, and 100 μg/mL streptomycin) containing M-CSF (25 ng/mL). Medium was changed every 2–3 days, and cells were well differentiated after one week. For in vitro M1 polarization, cells were treated with lipopolysaccharide (LPS, 1 μg/mL, Sigma-Aldrich, St Louis, MO) and IFN-γ (20 ng/mL, BD Bioscience, San Jose, CA) for 24 h; for M2 polarization, IL-4 (20 ng/mL, BD Bioscience, San Jose, CA) and IL-13 (20 ng/mL, BD Bioscience, San Jose, CA) were applied for 24 h. Human monocytic U937 cells were activated by PMA, 100 ng/mL for 48 h, to generate nonpolarized (Mo) macrophages and left untreated or polarized towards M1 using 100 ng/mL LPS and 20 ng/mL hIFNγ, or towards M2 using hIL-4 20 ng/mL and 20 ng/mL hIL-13 (PeproTech, Rocky Hill, NJ). RNA was extracted, reverse transcribed and analyzed by qPCR.

2.11. Hydrodynamic Transfection

MMP-12 cDNA was cloned into the pcDNA3 vector to generate pcDNA3-MMP12. The plasmids were purified using the QIAGEN Plasmid MAXI Kit (Qiagen, Hilden, Germany). Expression of MMP-12 was assessed by SDS-PAGE and Western blotting (not shown). Mice were treated for 6 weeks with CCl_4. At day 3 after the last CCl_4 injection wildtype mice were i.v. injected once with plasmid DNA (pcDNA3 empty vector or pcDNA3-MMP12, 10μg/20 g body weight) mixed with *TransIT*-QR Hydrodynamic Delivery Solution (Mirus, Madison, WI). Groups of three mice were sacrificed and analyzed either 48 h or 11 days after hydrodynamic injection, for assessment of in vivo transfection efficacy and for fibrosis assessment, respectively. Proteins were extracted from 100 mg liver using RIPA buffer (Cell Signaling, Danvers, MA) and cleared lysates resolved in a 4–10% polyacrylamide gel (Bis-Tris, Thermo Fischer, Waltham, MA), transferred to a PVDF membrane and detected with primary followed by secondary antibody (anti-MMP-12 1:1000, anti-tubulin 1:5000, goat and mouse secondary antibody 1:5000, all Santa Cruz Biotechnology, CA) followed by the Amersham ECL luminescence kit (GE, Chicago, IL).

2.12. Statistics

Data are shown as means ± SEM. Statistical differences were analyzed either with the 2-tailed unpaired Student's *t*-test (For comparison between two groups) or one-way analysis of variance (one-way ANOVA with Newman-Keuls' post-tests among multiple groups) using Graph pad Prism 5.0 (GraphPad software, La Jolla, CA).

3. Results

3.1. IL-4Rα Deficiency Retards Progression of Liver Fibrosis

Advanced liver fibrosis was induced in wildtype (WT) and IL-4Rα deficient (*Il4ra*$^{-/-}$) BALB/c mice by escalating doses of oral CCl_4 for 6 weeks. Mice receiving vehicle served as controls (Fig. S1A). In WT animals hepatic *Il4ra* transcripts increased >2-fold during progression (Fig. S1B). Morphometrical quantification of deposited collagen showed that after 6 weeks of progression *Il4ra*$^{-/-}$ mice developed significantly less fibrosis than their WT littermates (Fig. 1A). These results were confirmed by morphometrical quantification of alpha smooth muscle actin (α-SMA), by biochemical collagen (hydroxyproline, HYP) quantification and hepatic transcript levels of *Col1a1* (Fig. 1B–C; Fig. S1C). Serum ALT, a surrogate marker of liver inflammation, remained near normal during progression in *Il4ra*$^{-/-}$ mice as compared to a 3-fold increase in their WT controls (Fig. 1D). Collectively, these data provide in vivo evidence for an active role of overall IL-4Rα signaling in promoting liver inflammation and liver fibrogenesis during progression.

3.2. IL-4 and IL-13 Cytokines Are Important Drivers of Liver Fibrosis Progression

Both IL-4 and IL-13 can activate IL-4Rα signaling. To investigate whether loss of IL-4 and IL-13 will affect liver fibrosis progression, *Il4/Il13* double knockout (DKO) mice were subject to a 6-week course of CCl_4 treatment. Histological analysis revealed reduced liver fibrosis in the *Il4/Il13* DKO mice as demonstrated by Sirius Red and α-SMA staining (Fig. 1E; Fig. S1D), and by HYP determination (Fig. S1E). In line with this finding, compared to their WT controls, CCl_4-treated *Il4/Il13* DKO mice demonstrated a significant downregulation of serum ALT and of *Col1a1*, matrix metalloproteinase (*Mmp-8*, *-12* and *-13*) and tissue inhibitor of MMPs (*Timp-1*) transcripts (Fig. S1F; Fig. 1F–G). In *Il4ra*$^{-/-}$ mice numbers of IL-4- and IL-13-producing T cells were significantly reduced (Fig. S2A, B), proving that constitutive IL-4Rα deficiency reduces absolute T cells.

3.3. IL-4Rα Loss of Function Changes Liver Macrophage Populations During Liver Fibrosis Progression

In WT mice fibrosis induced by CCl_4 lead to an increase of hepatic but not splenic CD45^{+} immune cells in wildtype as well as *Il4ra*$^{-/-}$ mice (Fig. 2A, B). However, differences between WT and *Il4ra*$^{-/-}$ immune cells were found in the progression and early recovery phase of CCl_4-induced fibrosis, and evident in the hepatic B and CD4 T cell but not the CD8 T cell population (Fig. 2C).

Since monocyte-macrophages have been implicated as important regulatory cells in liver fibrosis progression and reversal, we focused on the effect of IL-4Rα signaling in monocytic (CD11b^{hi} F4/80^{int}) and resident (CD11b^{int} F4/80^{hi}) macrophages. FACS analysis demonstrated that IL-4Rα deletion lead to a significant decrease of resident macrophages in the vehicle treated control group (Fig. 2D). Moreover, upon CCl_4 treatment the increase of pro-inflammatory Ly-6C^{hi} monocytic

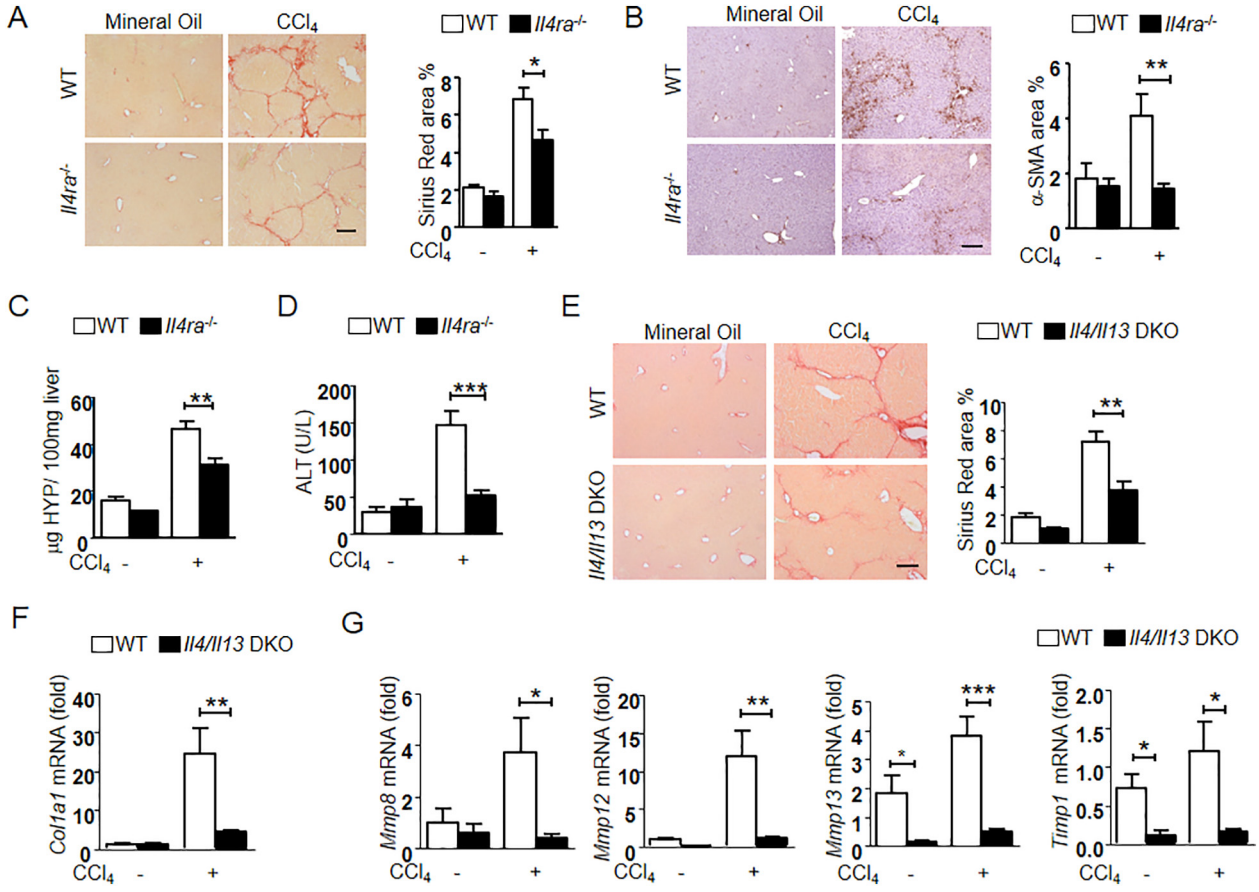

Fig. 1. Loss of IL-4Rα signaling retards liver fibrosis progression. (A–D) *Il4ra*$^{-/-}$ and WT mice received CCl_4 or vehicle (mineral oil) for 6 weeks by oral gavage. (A–B) Representative (A) Sirius Red and (B) α-smooth muscle actin (α-SMA) staining of WT and *Il4ra*$^{-/-}$ liver sections; bar: 200 μm. The diagrams depict mean percentages of stained areas from 10 microscopic fields of each mouse (n = 6 per group). (C) Total liver collagen (hydroxyproline, Hyp). (D) Serum alanine aminotransferase (ALT) levels in WT (white bars) and *Il4ra*$^{-/-}$ (black bars) mice with or without CCl_4 treatment (n = 6 per group). (*E*-G) *Il4/Il13* DKO and WT type mice received CCl_4 or vehicle (mineral oil) for 6 weeks by oral gavage. (E) Representative Sirius Red staining (n = 5) of WT and *Il4/Il13* DKO liver sections; bar: 200 μm. The diagrams depict mean percentages of stained areas from 10 microscopic fields of each mouse. (F) *Col1a1* mRNA (normalized to *Gapdh* mRNA, n = 5). (G) Hepatic transcript levels of *Mmp8*, *12* and *13* and *Timp1* in mice received vehicle or CCl_4 (n = 5). $^{*}p < 0.05$, $^{**}p < 0.01$, $^{***}p < 0.005$ (unpaired Student's *t*-test). All data are expressed as means ± SEM. Results are representative of two independent experiments.

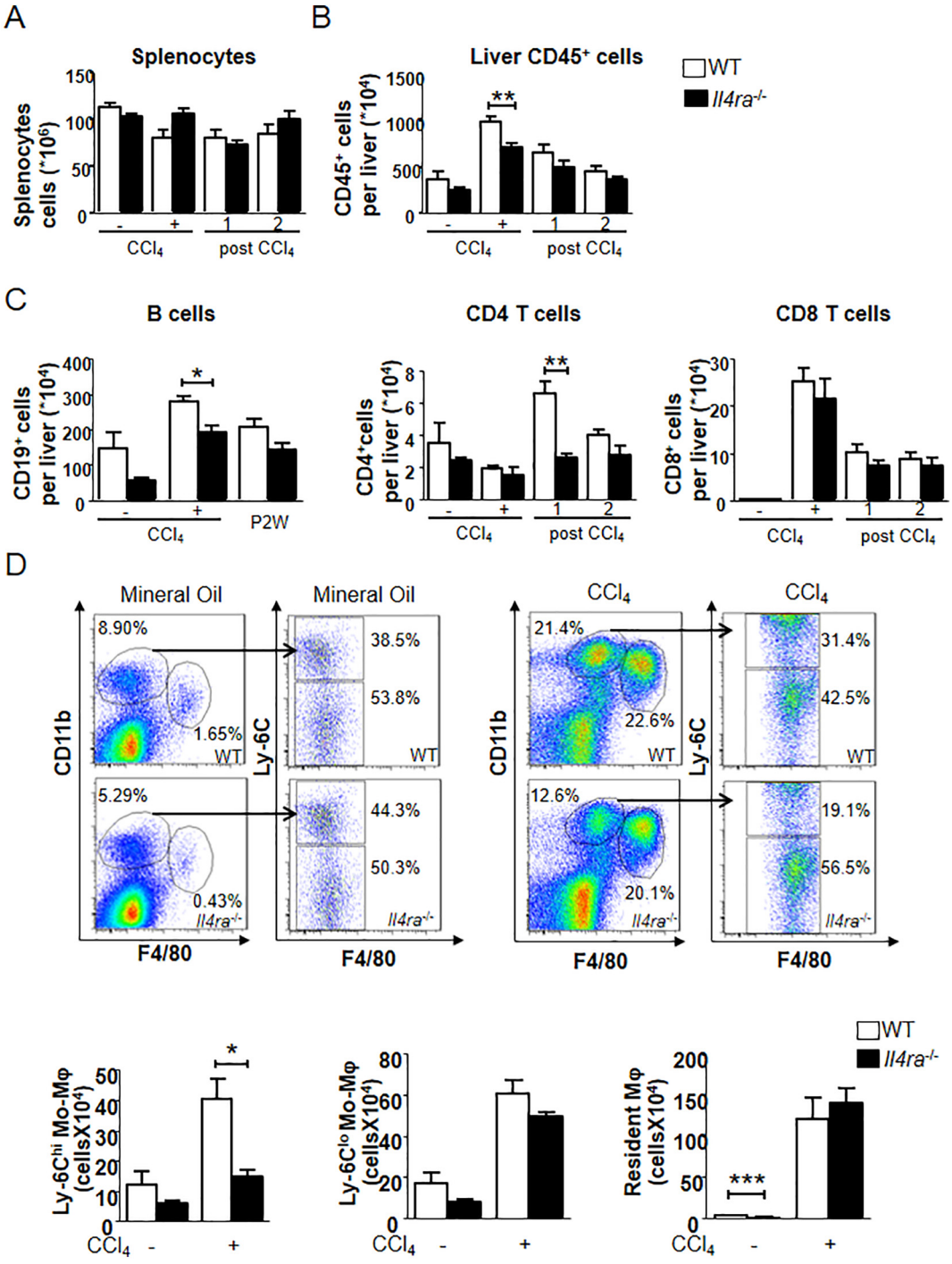

Fig. 2. IL-4Rα is required for infiltration by monocyte-derived inflammatory macrophages (Ly-6C^{hi} CD11b^{hi} F4/80^{int}). Bar diagrams indicating absolute (A) splenic CD45^{+}, and (B) hepatic CD45^{+}, (C) CD19^{+} (B cell), CD4 and CD8 T cell numbers of WT and *Il4ra*$^{-/-}$ mice that had received either mineral oil or CCl_4 for 6 weeks. Analysis was performed one day, one and two weeks after CCl_4 withdrawal (n = 4 per group). (D) Representative FACS plots showing liver monocytes/macrophages (see also Fig. S2) of WT and *Il4ra*$^{-/-}$ mice that were analyzed at the end of 6 weeks of treatment with CCl_4. In the two plots on the left resident macrophages (CD11b^{int} F4/80^{hi}) and monocytes/macrophages (CD11b^{hi} F4/80^{lo}) are shown. CD11b^{hi} F4/80^{lo} cells were further subdivided into pro-inflammatory (Ly-6C^{hi}) and anti-inflammatory (Ly-6C^{lo}) monocytes/macrophages. Bar diagrams show the mean numbers of monocytes/macrophages per liver (n = 4 per group). *p < 0.05, **p < 0.01, ***p < 0.005 (unpaired Student's *t*-test). All data are expressed as means ± SEM. Results are representative of ≥2 independent experiments.

macrophages was significantly attenuated in livers of *Il4ra*$^{-/-}$ mice (Fig. 2D; Fig. S3A–G).

3.4. IL-4Rα Signaling Does Not Contribute to Fibrosis in a Model of Severe Non-alcoholic Steatohepatitis

Severe hepatocyte lipoapoptosis was induced in mice receiving the MCD diet for 8 weeks. Liver collagen was increased 4-fold in wild type mice, but fibrosis was not attenuated in *Il4ra*$^{-/-}$ mice, different from mice with CCl_4-induced liver fibrosis (Fig. S4A, B). Notably, there was a downregulation of *Il4ra* in wildtype mice on the MCD vs the control MCS diet, in contrast to mice with CCl_4-induced liver fibrosis, and as expected its complete absence in the *Il4ra*$^{-/-}$ mice (Fig. S4C). Moreover, IL-4Rα deletion did not affect macrophage CD68 expression, as in the CCl_4 as above model, indicating a less important role of this receptor in fibrosis progression in this model (Fig. S4C).

3.5. IL-4Rα as a Therapeutic Target for Treating Liver Fibrosis In Vivo

We used optimized antisense oligonucleotides (ASOs) to the *Il4ra* gene with high hepatic delivery (Kurreck et al., 2002; Lee et al., 2013) that were first tested in vitro on RAW murine macrophages to demonstrate a robust target knockdown compared to a negative control ASO (Fig. S5A). For in vivo studies we chose ASO2 for its stronger inhibition of IL-4Rα expression (Fig. S5B). ASOs were applied during CCl_4-induced fibrogenesis for 3 weeks (Fig. 3A). During progression, therapy with ASO2 strongly inhibited hepatic collagen deposition (Fig. 3B) which was accompanied by a significant suppression of *Col1a1*, *α-SMA* and *Tgfb-1* transcripts (Fig. 3D). Moreover, ASO2 significantly reduced the number of liver $CD68^+$ macrophages and levels of *Cd68*, *iNOS* and *Mrc1* transcripts (Fig. 3C and E). Taken together, IL-4Rα appears instrumental in increasing the influx of monocyte-macrophages.

3.6. Loss of IL-4Rα Signaling in T Cells Does Not Alleviate Toxin-induced Liver Fibrosis

IL-4Rα signaling and the associated Th2 T cell response are drivers of portal liver fibrosis induced by Schistosomal parasites (Chiaramonte et al., 1999; Pesce et al., 2009). To study the role of T cell IL-4Rα in our model of parenchymal fibrosis progression and reversal, mice with a T cell-specific IL-4Rα deletion ($Il4ra^{\Delta CD4}$) were generated and analyzed in the progression model. Quantitative PCR and flow cytometry demonstrated a significant reduction of IL-4Rα in $CD4^+$ T cells of $Il4ra^{\Delta CD4}$ mice (Fig. S6A–B), whereas several fibrosis related readouts showed no

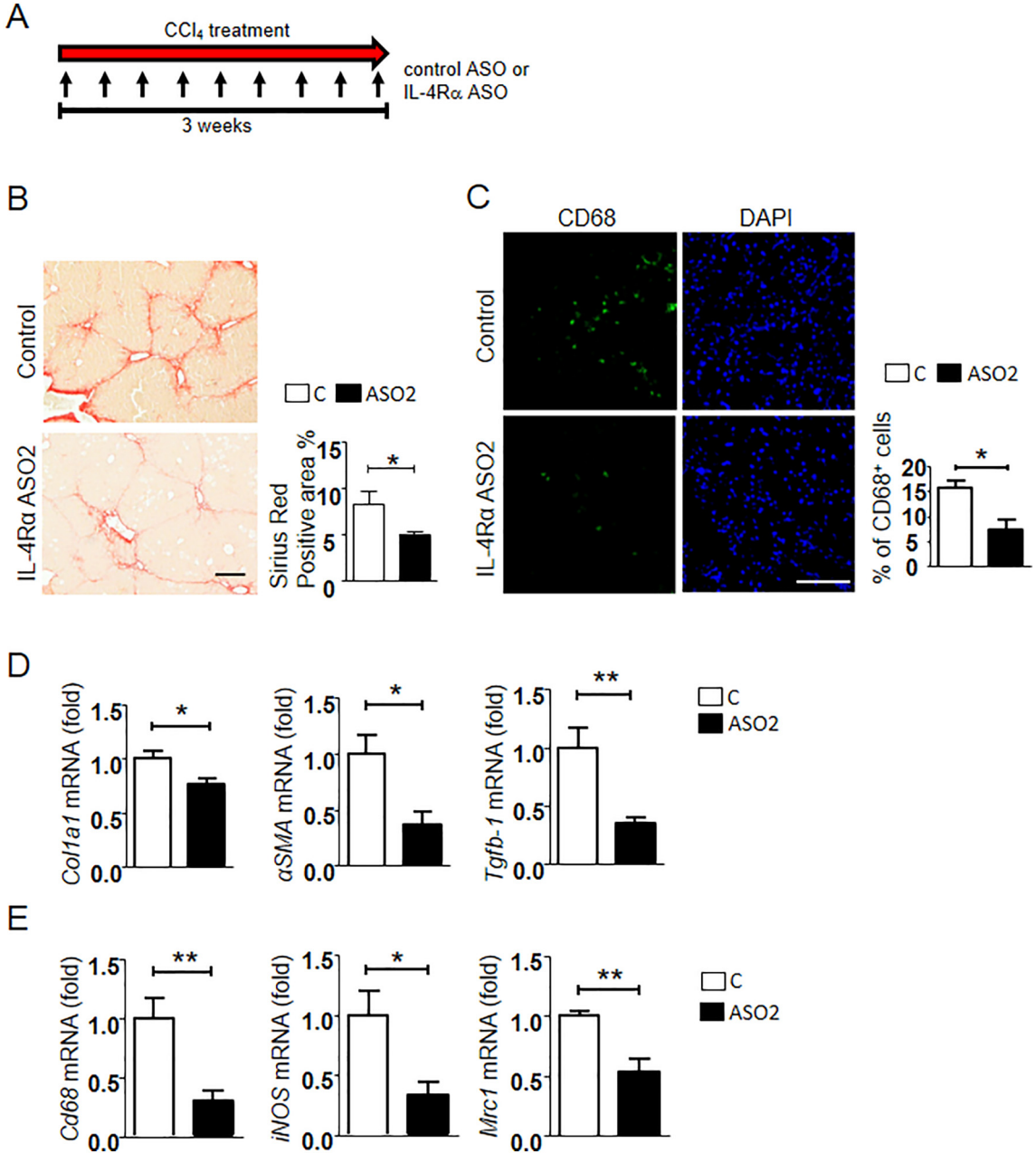

Fig. 3. Inhibition of IL-4Rα expression by specific antisense oligonucleotides decreases fibrosis progression. (A) Mice received 9 doses of either control oligonucleotide (C) or IL-4Rα-ASO2 during three weeks of CCl_4 treatment. (B) Sirius Red and (C) CD68 (macrophage) staining in livers of mice with fibrosis progression. Bar: 200 and 50 μm, respectively (n = 4–5). (D) Relative hepatic transcript levels of key fibrosis-related genes in CCl_4-treated mice receiving either the control oligonucleotide or the IL-4Rα-specific ASO2. (E) Transcript levels for macrophage marker genes (*Cd68*, *Mrc1* and *iNOS*) for control oligonucleotide- and IL-4Rα-specific ASO2-treated livers during fibrosis progression (n = 5). $^*p < 0.05$, $^{**}p < 0.01$ (unpaired Student's *t*-test). All data are expressed as means ± SEM. Data are representative of three independent experiments.

difference between control and *Il4ra*$^{\Delta CD4}$ mice (Fig. S6C–E). Collectively, this indicates that IL-4Rα signaling in T cells does not affect parenchymal liver fibrosis progression or reversal.

3.7. Myeloid Cell-Specific Deletion of IL-4Rα Attenuates Fibrosis Progression

To address the role of macrophage IL-4Rα in liver fibrosis progression, we generated mice with myeloid-specific IL-4Rα deletion (*Il4ra*$^{\Delta LysM}$). When these mice were subject to 6 weeks of CCl_4, total hepatic *Il4ra* expression was significantly suppressed compared to control mice, with analysis shortly after the last dose of CCl_4 (Fig. S6F). Comparable to our findings in general *Il4ra*$^{-/-}$ mice, Sirius Red and α-SMA staining, HYP content and *Col1a1* expression showed attenuated liver fibrogenesis and decreased ALT levels in *Il4ra*$^{\Delta LysM}$ compared to *Il4ra*$^{fl/-}$ control mice (Fig. 4A–D). These results indicate that IL-4Rα signaling through myeloid but no other hepatic cells plays an important regulatory role in liver fibrosis progression.

3.8. IL-4Rα Is Specifically Deleted in Resident Macrophages in *Il4ra*$^{\Delta LysM}$ Mice during CCl_4-induced Liver Fibrosis

A prior study showed that deletion of IL-4Rα in *Il4ra*$^{\Delta LysM}$ in a Schistosomiasis model was incomplete (Vannella et al., 2014). To unambiguously define the cell type that drives IL-4Rα-mediated liver fibrogenesis during progression, the number of myeloid lineage cells and their expression of IL-4Rα were investigated (Figs. S6G and S7A, B). We could demonstrate that the abrogation of IL-4Rα, as mediated by LysM-Cre, was highly efficient in resident macrophages (CD11b^{int} F4/80^{hi}), but insignificant in neutrophils or Ly-6C^{hi} or Ly-6C^{lo} monocytic macrophages (CD11b^{hi} F4/80^{lo}) (Fig. S7A, B). Refined FACS analysis showed a decreased expression of MHC class II and CD86 on these resident macrophages in *Il4ra*$^{\Delta LysM}$ mice compared to control mice. This suggests that the attenuated liver fibrosis in IL-4Rα deleted mice may be largely due to fewer pro-inflammatory resident macrophages (Fig. S7C), but also to fewer freshly recruited monocyte-macrophages which apparently were only affected by the general IL-4Rα deletion (see Fig. 2D).

In line with these findings, qPCR and immunohistochemical analysis of livers of *Il4ra*$^{\Delta LysM}$ mice, with a macrophage specific IL-4Rα deletion, showed a reduction of overall macrophages (CD68^{+}), and of putative M1-, but to a lesser degree also of M2-type populations, accompanied by a decrease of *Tgfb1* (profibrotic), *iNOS* and *Il1b* (M1), *Arg1*, *Mrc1* and YM1 (M2) shortly after termination of 6 weeks of CCl_4, when features of both progression and early reversal may coexist (Fig. 5A–B).

We therefore conclude that liver fibrosis progression is mediated by IL-4Rα partly through enhanced pro-inflammatory conversion of resident macrophages. There is also a reduction of M2-type macrophage markers in *Il4ra*$^{\Delta LysM}$ mice during progression and early reversal (3 days after cessation of CCl_4) which likely impacts the fibrogenic over the fibrolytic response.

3.9. Loss of IL-4Rα Reduces M2-type Macrophage Subsets and Retards Spontaneous Liver Fibrosis Regression

To study the role of IL-4Rα in longer-term fibrosis reversal, we used a model of spontaneous fibrosis regression (6 weeks of CCl_4 followed by 2 or 4 weeks without treatment), where fibrolytic macrophages play an important role (Fig. S8A). As shown in Fig. S8B–D, approx. 30% of total liver collagen deposition had disappeared after 2 weeks off CCl_4 in WT mice, whereas fibrosis resolution was retarded in *Il4ra*$^{\Delta LysM}$ mice (Fig. 6A). This divergent effect during reversal vs progression was further confirmed in a second experiment showing elevated *Col1a1* and *α–SMA* transcript levels in *Il4ra*$^{\Delta LysM}$ vs the IL-4Rα expressing mice (Fig. 6B).

To confirm the translational relevance of these findings, we designed a pharmacological intervention using a specific IL-4Rα ASO to fibrotic WT mice during the reversal phase (Fig. 6C). Here, ASO2 significantly attenuated resolution, as shown by a relative increase of liver collagen and *Col1a1* mRNA expression vs mice treated with a scrambled control ASO (Fig. 6D–E). Moreover, ASO2 significantly reduced the protein product of the Mrc1 gene (CD206)$^{+}$ M2-type macrophage numbers and suppressed the M2-related genes *Mrc1* and *Arg1*, without affecting M1-related *iNos* mRNA (Fig. 6F–G) .

These results consistently showed that IL-4Rα regulates liver fibrosis differently in fibrosis progression vs fibrosis reversal, and that this effect is largely mediated by macrophages and no other IL-4Rα expressing cells such as T cells or hepatocytes.

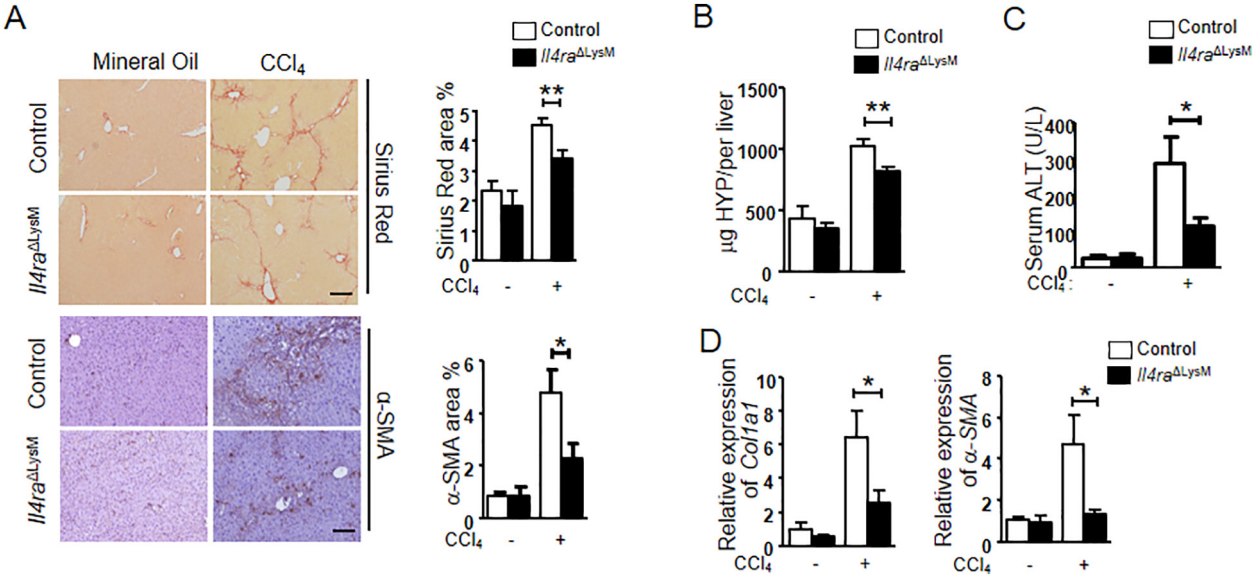

Fig. 4. Myeloid IL-4Rα deficiency attenuates CCl_4-induced liver fibrosis. Il4ra$^{f/-}$ (control) and myeloid cell IL-4Rα-deleted (*Il4ra*$^{\Delta LysM}$) mice were treated with CCl_4 for 6 weeks. Mice were analyzed 3 days after the last dose of CCl_4. (A) Representative Sirius Red (upper) and α-SMA (lower) stained sections of CCl_4 treated mice. Bar: 200 μm. The diagrams on the right depict mean percentages of stained areas from 10 microscopic fields per liver (n = 5). (B) Hepatic hydroxyproline (Hyp) levels (n = 5). (C) Serum ALT levels of control and *Il4ra*$^{\Delta LysM}$ mice (n = 5). (D) Hepatic *Col1a1* and *α-SMA* transcript levels (n = 5). Transcript levels were normalized to *Gapdh* mRNA. *p < 0.05, **p < 0.01 (unpaired Student's *t*-test). All data are expressed as means ± SEM. Results are representative of two independent experiments.

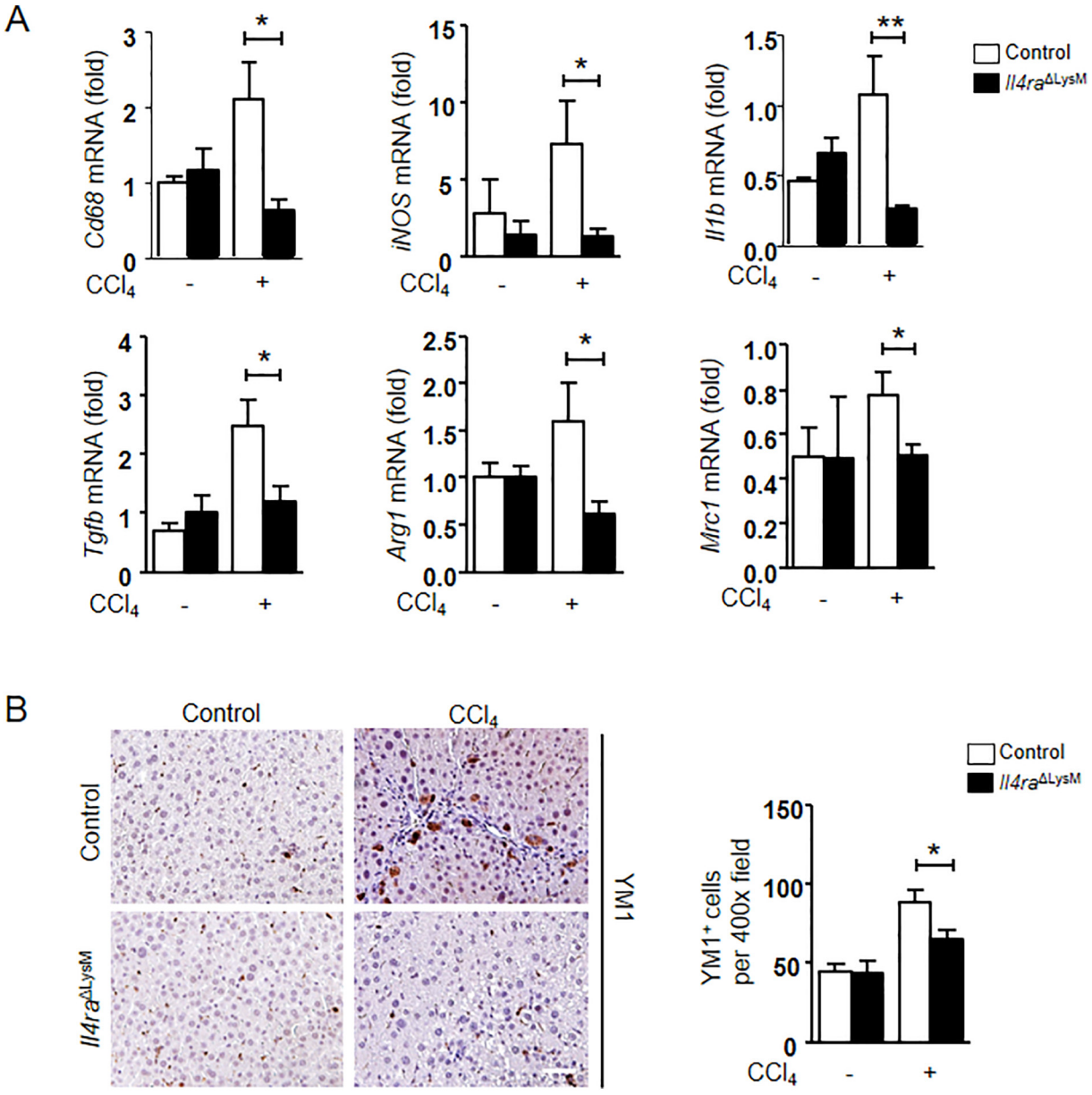

Fig. 5. Reduction of both M1- and M2-type macrophage markers in *Il4ra*$^{\Delta LysM}$ mice during CCl_4-induce liver fibrosis. (A) Transcript levels of *Cd68*, *iNOS*, *Il1b*, *Tgfb1*. *Arg1* and *Mrc1* in control and *Il4ra*$^{\Delta LysM}$ mice treated with mineral oil or CCl_4 for 6 weeks (n = 5). (B) Representative YM1 immunohistochemistry in control and *Il4ra*$^{\Delta LysM}$ mice treated with mineral oil or CCl_4 for 6 weeks (n = 5). Bar: 50 μm. *p < 0.05, **p < 0.01 (unpaired Student's *t*-test). All data are expressed as means ± SEM.

3.10. IL-4Rα Signals Through STAT6 to Induce Fibrolytic Matrix Metalloproteinase Expression in Macrophages

MMPs are instrumental in ECM remodeling and fibrosis regression. We therefore studied the expression of a panel of MMPs during early fibrosis reversal in control and *Il4ra*$^{\Delta LysM}$ livers. In early reversal, at 24 or 72 h after CCl_4 withdrawal, expression of *Mmp12*, *14*, *16* and *20* mRNA was increased. At 72 h *Mmp16* and *20*, and especially *Mmp12* transcripts were significantly suppressed in *Il4ra*$^{\Delta LysM}$ compared to control livers (Fig. 7A and see also the Supplemental Information).

To study how far IL-4Rα signaling could directly potentiate the expression of *Mmp12* in M2-type macrophages in vitro, peritoneal and bone marrow-derived macrophages (BMDM) from WT and *Il4ra*$^{-/-}$ mice were isolated and polarized with either IL-4 and/or IL-13 for 24 h. M2 related *Mrc1* and *Arg1* transcripts were up-regulated in WT but not *Il4ra*$^{-/-}$ macrophages in response to IL-4 and IL-13 (Fig. S9A–B), suggesting that WT but not *Il4ra*$^{-/-}$ macrophages can be differentiated into M2-type macrophages in vitro. *Mmp12* transcripts were prominently induced in both primary WT but not *Il4ra*$^{-/-}$ macrophages after incubation with IL-4 and/or IL-13 (Fig. 7B–C). Moreover, human MMP-12 expression was dramatically increased in PMA-activated U937 monocytes that were treated with M2 (human IL-4 and IL-13) but not M1 cytokines (LPS and human IFNγ) (Fig. S9C). Moreover, M1-polarized (LPS and IFNγ-treated) WT and *Il4ra*$^{-/-}$ BMDM did not show significant differences in their low level of *Mmp12* expression (Fig. S10A).

Phospho-STAT6 is a major downstream signal transducer for IL-4/IL-13-dependent genes (Lin et al., 1995). In hepatic macrophages lacking IL-4Rα, there was suppressed induction of phospho-STAT6 in response to IL-4 or IL-13 during fibrosis progression (Fig. 7D). In this vein, ASOs targeting the IL-4Rα and STAT6 genes significantly down-regulated *Mmp12* mRNA in RAW macrophages (Fig. 7E). No direct connection was found between M1 cytokines and MMP-12 expression and stimulation of macrophages with LPS did not enhance *Mmp12* expression, neither in wildtype nor in IL-4Rα deleted cells (Fig. S10A). However, we found decreased pSTAT3-activation in hepatic macrophages isolated from mice with CCl_4

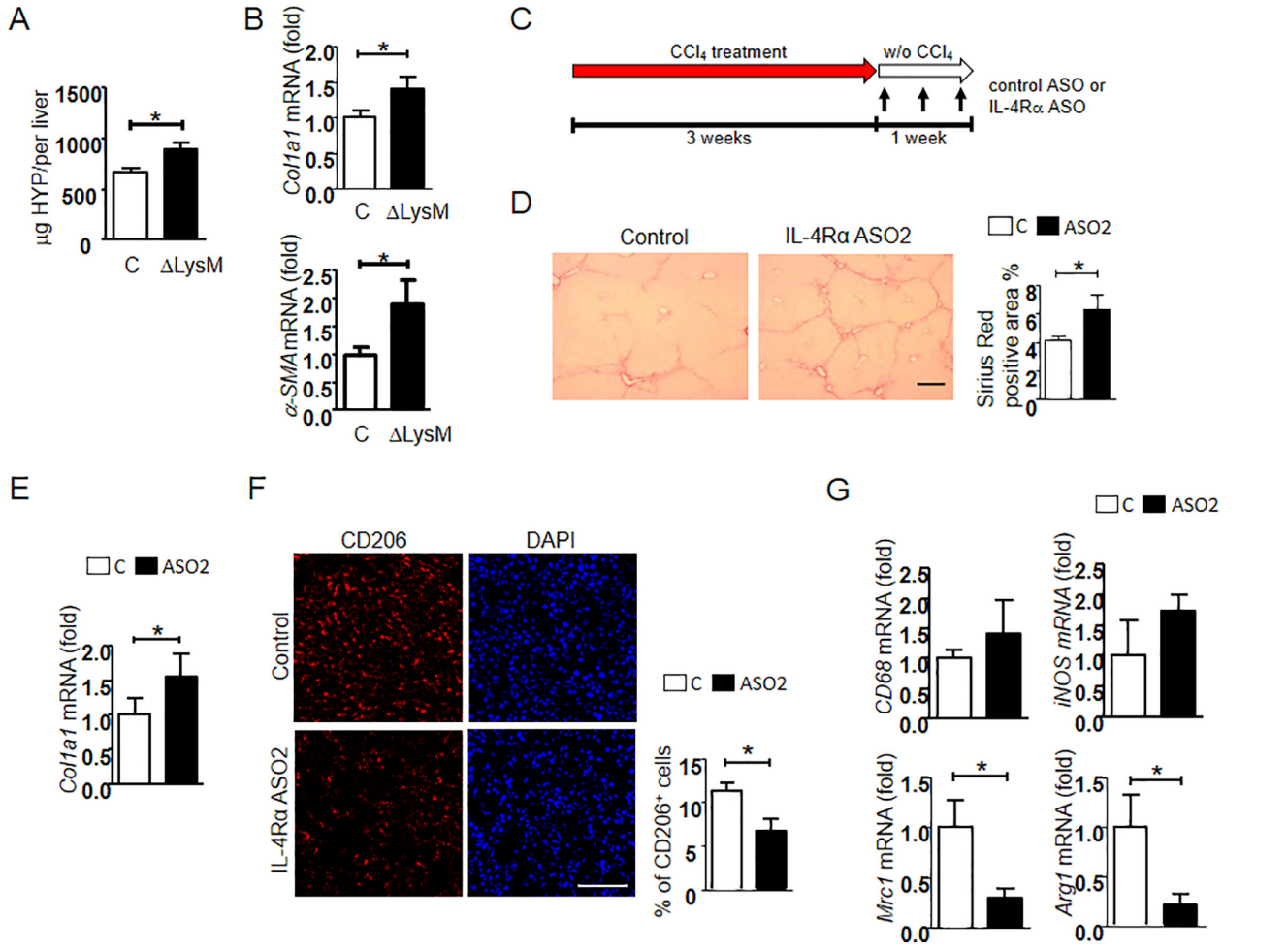

Fig. 6. IL-4Rα antisense oligonucleotides attenuate resolution and inhibit M2-type polarization during spontaneous fibrosis reversal. (A) Liver Hyp level of control and *Il4ra*$^{\Delta LysM}$ mice after 2 weeks of CCl_4 withdrawal (n = 5). (B) Transcript levels of *Col1a1* and *α-SMA* of control and *Il4ra*$^{\Delta LysM}$ mice after 2 weeks of CCl_4 withdrawal (n = 6). (C–G) ASO2-mediated IL-4Rα reduction caused the retardation of fibrosis reversal. (C) Mice received 3 doses of control oligonucleotide or ASO2 during the first week of reversal, off CCl_4. Mice were analyzed one day after the last dose of ASO2. (D) Representative Sirius Red staining in livers of mice during the reversal phase (n = 6). Bar: 200 μm. Bar diagrams represent results from 10 microscopic fields per liver. (E) Transcript levels for *Col1a1*. (F) Representative CD206 (M2-type macrophage) staining in livers of mice during the reversal phase (n = 6). Bar: 50 μm. Bar diagrams represent results from 10 microscopic fields per liver. (G) Transcript levels for macrophage specific genes (*Cd68*, *Mrc1*, *Arg1* and *iNOS*, n = 4). *p < 0.05 (unpaired Student's t-test). All data are expressed as means ± SEM. Results are representative of ≥2 independent experiments.

fibrosis that lacked IL-4Rα and which were stimulated with IL-6 (Fig. S10B).

To confirm that MMP-12 functions as an inducer of fibrolysis during fibrosis reversal, an empty vector or a vector containing *Mmp12* cDNA was delivered into fibrotic livers during the reversal phase using hydrodynamic transfection (Fig. S10C). Sirius Red staining showed that *Mmp12* cDNA but not the empty vector induced fibrosis resolution (Fig. 7F). These results identify MMP-12 (and to a lesser degree MMP-16 and -20) as primary bona fide mediator(s) of M2-type macrophage-mediated fibrolysis during the early phase of reversal.

In summary, inhibition of IL-4Rα expression ameliorated the progression but retarded regression of parenchymal liver fibrosis. Therefore, targeting the IL-4Rα appears to be a therapeutic option for patients with progressive liver fibrosis, but may retard resolution when the inflammatory triggers are absent.

4. Discussion

IL-4 and IL-13 and their common receptor subunit IL-4Rα play a central role in M2-type macrophage and Th2 cell polarization which are held responsible for the promotion of organ fibrosis. Thus an IL-4 neutralizing antibody or the dominant negative IL-13Rα1/2 antagonist sIL-13Rα2-Fc reduced fibrosis in the mouse model of hepatic Schistosomiasis (Cheever et al., 1994; Chiaramonte et al., 1999). Here we demonstrate that, unexpectedly, IL-4Rα on macrophages promotes both hepatic inflammation and fibrosis during progression, while it permits unrestricted fibrosis resolution during spontaneous reversal. Notably, we showed that other cells than macrophages (Bhattacharjee et al., 2013; Stein et al., 1992) or T cells (Cheever et al., 1994; Chiaramonte et al., 1999) that can respond to IL-4 and IL-13, such as mast cells (Nilsson and Nilsson, 1995; Ochi et al., 2000), eosinophils(Hao et al., 2000; Sher et al., 1990; Tomkinson et al., 2001), (myo-)fibroblasts (Chandriani et al., 2014), and liver epithelial cells (Richter et al., 2001), did not significantly contribute to liver inflammation or fibrosis, which is strongly supported by our data demonstrating that the macrophage specific IL-4Rα-deletion (*Il4ra*$^{\Delta LysM}$) yielded similar results as mice with the general IL-4Rα-knockout, with the exception that it did not affect the freshly recruited monocyte-macrophages, as observed in mice with the general IL-4Rα. We also demonstrate that, conversely, macrophage IL-4Rα signaling can also promote liver fibrosis regression via STAT6-dependent transcriptional activation of *Mmp12*, and that pharmacological inhibition of IL-4Rα recapitulated the functional effects of genetic IL-4Rα deletion.

Schistosomiasis is associated with a prominent infiltration by Th2 cells. While these cells promote fibrogenesis, they also secrete IL-4 and IL-13 that was shown to induce an anti-inflammatory and antifibrotic M2-type macrophage phenotype (Herbert et al., 2004;

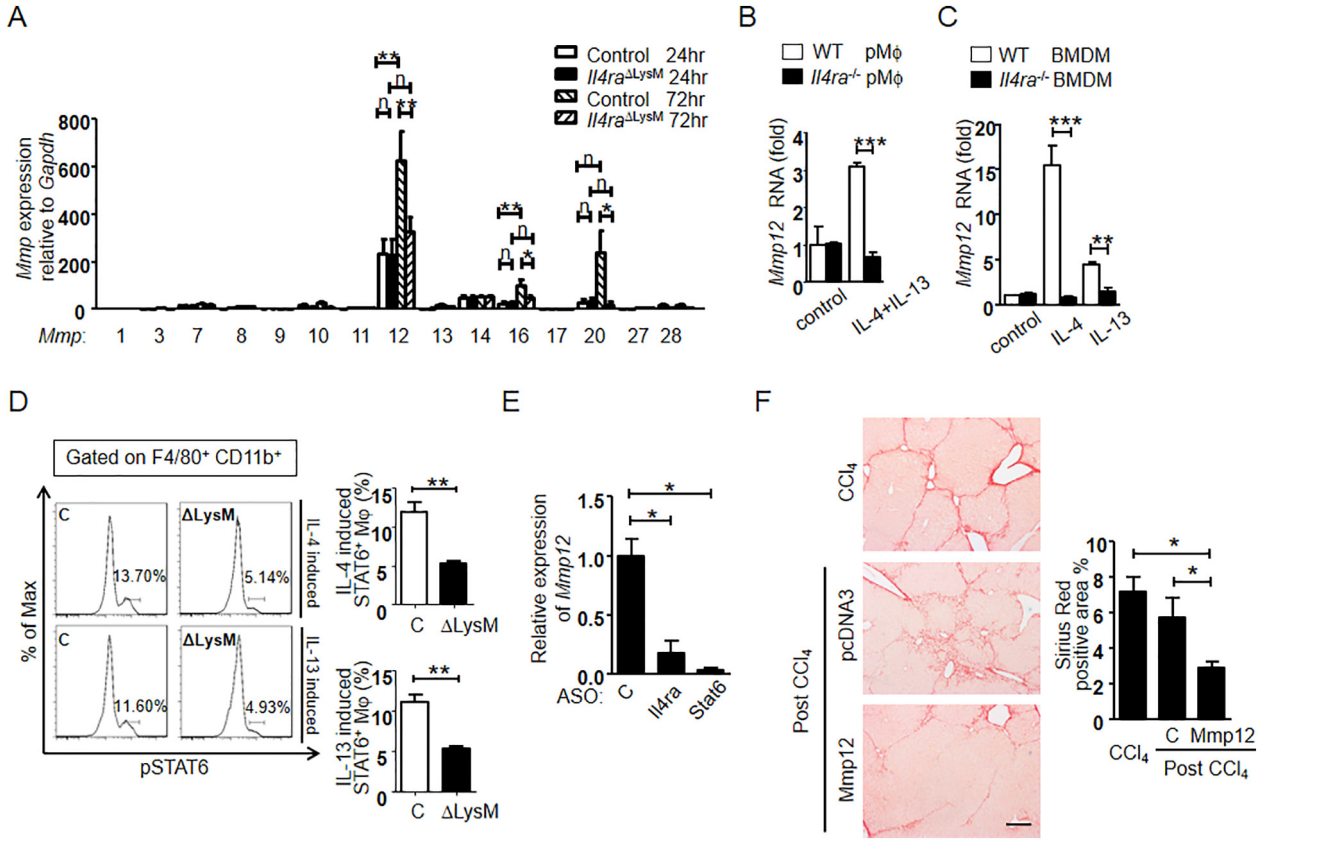

Fig. 7. IL-4 and IL-13 mediated STAT6 activation induces macrophage MMP-12 expression. (A) Relative *Mmp* transcripts (normalized to *Gapdh* RNA) in livers of control and *Il4ra*$^{\Delta LysM}$ mice that were analyzed at 24 h and 72 h after 6 weeks of CCl_4-treatment (n = 5). *p < 0.05, **p < 0.01; n, not significant (one-way ANOVA). (B,C) Peritoneal macrophages (pMφ) or bone marrow-derived macrophages (BMDM) were either untreated or treated with IL-4 (20 ng/mL) and/or IL-13 (20 ng/mL) for 24 h. *Mmp12* transcript were measured (n = 4 per group). (D) Immune cells from *Il4ra*$^{fl/-}$ control (C) and *Il4ra*$^{\Delta LysM}$ (ΔLysM) livers were harvested at day three following CCl_4 treatment and stimulated with IL-4 or IL-13 for 30 min for the detection of phospho-STAT6 in macrophages (n = 4 per group). (E) *Mmp12* transcript levels in RAW264.7 macrophages transfected with the indicated oligonucleotide. (F) Representative Sirius Red staining of liver sections from mice three days after 6 weeks of fibrosis induction with CCl_4 or from mice after 2 weeks of recovery after the last CCl_4 dose. Mice in the reversal group were injected with empty pcDNA3 vector (C) or pcDNA3-MMP12 (Mmp12). Bar diagrams show the quantification results. Bar: 200 μm. *p < 0.05, **p < 0.01, ***p < 0.005 (unpaired Student's *t*-test). All data are expressed as means ± SEM. See also the supplemental table of Mmp transcript levels.

Kaplan et al., 1998; Pesce et al., 2009). This was confirmed by *Il4ra*$^{\Delta LysM}$ mice with chronic Schistosomiasis that showed increased liver inflammation and fibrosis (Vannella et al., 2014). However, the role of these cytokines and especially of IL-4Rα signaling in non-parasitic hepatic liver disease, which is the prominent cause of liver fibrosis, had not been addressed. While the innate immune response by monocytes/macrophages and neutrophils usually precedes (T cell mediated) adaptive immunity (Campbell et al., 1981; Tacke and Zimmermann, 2014), both the choice of the in vivo model and the timing of organ damage or regeneration may determine how far Th2 cells or M2-type macrophages are primary drivers of inflammation or fibrosis. Th2 T cells are important sources of IL-4, which together with IL-13 is the major ligand for IL-4Rα. A recent paper indicated that IL-13 was produced by type 2 innate lymphoid cells (ILC-2) cells upon exposure to IL-33; however, the deletion of ILC-2 under CCl_4 treatment did not completely rule out the participation of Th2 cells (McHedlidze et al., 2013). Thus we generated *Il4ra*$^{\Delta CD4}$ knockout mice to exclude a role of Th2 cells in the CCl_4 model of parenchymal liver fibrosis, which had not been studied before. In line with the major finding of the paper by McHedlidze, the *Il4ra*$^{\Delta CD4}$ knockout showed no difference compared to the wildtype control mice under CCl_4 treatment. Another recent study showed that IL-4 drives the expression of surfactant protein SP-A in the lung and of complement component C1q in the liver and peritoneal cavity, which amplify IL-4Rα signaling in type-2 infectious models in these organs (Minutti et al., 2017). It should be of interest to study how far C1q may also be involved in our noninfectious liver fibrosis models. We have measured hepatic C1q transcripts at peak fibrosis and on days 1 and 3 of reversal. Here we could not find significant differences between control and *Il4ra*$^{\Delta LysM}$ mice.

Our finding of a pro-inflammatory and pro-fibrogenic role of IL-4Rα signaling during fibrosis progression, in contrast to its anti-inflammatory and fibrolytic role during regression, relativates prior results with IL-4, IL-13 or IL-13Rα2 in the models of pulmonary (Chandriani et al., 2014), (Schistosomal) liver (Cheever et al., 1994; Chiaramonte et al., 1999; Kaviratne et al., 2004) and intestinal fibrosis (Fichtner-Feigl et al., 2007; Fichtner-Feigl et al., 2006), models that solely represent progression. These settings are also different from human (liver) fibrosis which is characterized by foci or waves of progression and reversal, even in advanced fibrosis (Wanless et al., 2000), features that can only be represented by progression and reversal models as employed by us (Issa et al., 2004; Popov et al., 2011). Finally, parenchymal rather than portal liver fibrosis determines the degree of liver dysfunction and failure (Schuppan and Afdhal, 2008). Our data also suggest that IL-4Rα signaling in macrophages may be an important regulator of inflammation and fibrosis in the prevalent cases with parenchymal as opposed to portal liver fibrosis.

Accordingly, therapeutic intervention targeting the IL-4Rα with a specific antisense oligonucleotide that intrinsically addresses the liver and preferentially macrophages (Butler et al., 2000) generated the same effects as the macrophage specific (or constitutive) knockout of IL-4Rα in the fibrosis models, as also shown by correlative comparison of the change in fibrosis and the number and subtype of macrophages

during the progression and reversal phase under CCl_4 treatment. This may suggest a prediction about the antifibrotic efficacy in patients with liver fibrosis when either an IL-4Rα ASO or a dual human IL-4/IL-13 blocking antibody, which has already entered the clinic and which was developed for the treatment of asthma (Friedman et al., 2013; Mehal and Schuppan, 2015; Schuppan and Kim, 2013), would be applied. Since therapeutic silencing of the IL-4Rα could be beneficial for other inflammatory diseases such as ulcerative colitis, systemic sclerosis and cancer, our findings may have broader translational implications.

Somewhat unexpectedly, ablation of IL-4Rα signaling during fibrosis progression not only reduced the number of hepatic M2-type macrophages, B and $CD4^+$ T cells, but also increased pro-inflammatory (Ly-$6C^{hi}$ $CD11b^+$ $F4/80^{int}$) macrophages. This indicates that IL-4Rα signaling may increase not only monocyte recruitment but also potentiate the transition from these proinflammatory monocytes to early forms of monocytic macrophages. On the other hand, during reversal, IL-4Rα deficiency reduced the number of the M2-type, potentially antifibrotic (restorative) subset of Ly-$6C^{lo}$ $CD11b^+$ $F4/80^{int}$ macrophages, likely including resident macrophages, that may be mainly responsible for fibrolytic remodeling (Madsen et al., 2013; Ramachandran et al., 2012). Here we also show that fibrolysis was accompanied by STAT6-dependent upregulation of macrophage *Mmp12* expression, an enzyme which is specifically degrading elastin and collagens (Pellicoro et al., 2012), major components of hepatic scar tissue.

Overall, blockade of IL-4Rα signaling has an anti-inflammatory and anti-fibrotic effect during toxin-induced liver fibrosis progression and retards - but does not prevent - fibrosis resolution. Since these context- and stage-specific in vivo effects of IL-4Rα signaling in parenchymal liver fibrosis are mediated by macrophages and closely linked to macrophage numbers and polarization, macrophage-targeted antifibrotic therapies will likely need to be adjusted to the etiology and (inflammatory) activity of the underlying liver disease.

Financial Support

The project was supported by an ERC Advanced Grant ERC-2011-ADG_20110310 of the EU to D.S. and a fellowship by the National Science Council (NSO) Taiwan to S.W.

Author Contributions

S.W. designed, performed and analyzed the majority of experiments, and drafted the manuscript. X.W., K.P. and T.C. performed mouse studies, collagen assessment, serum measurements and qPCR analysis; Y.T. and A.W. supported cell isolation, staining and flow cytometry, and supported drafting the manuscript; S.V. and K.P. supported the mouse studies, immunohistochemical and immunofluorescence analyses; Y.O. supported mouse studies and fibrosis assessments; T.R. optimized hydrodynamic injections; O.M. performed mouse genotyping and analytical studies; T.B. and H.S. provided advice and helped draft the manuscript; F.B. provided $LysM^{Cre}$ and IL-4Rα mutant mice and gave valuable advice; J.R.C. and M.L.M. designed, produced and optimized antisense oligonucleotides; E.B. helped in data interpretation and writing the manuscript; D.S. designed, planned and interpreted the studies and wrote the manuscript.

Competing Interests

The authors declare no competing financial interests.

Acknowledgments

We thank Dennis Strand for setting up the confocal microscope, and Alexei Nikolaev for the technical work regarding immunofluorescence staining of liver tissues.

Appendix A. Supplementary Data

Supplementary data to this article can be found online at https://doi.org/10.1016/j.ebiom.2018.01.028.

References

Barron, L., Wynn, T.A., 2011. Fibrosis is regulated by Th2 and Th17 responses and by dynamic interactions between fibroblasts and macrophages. Am. J. Physiol. Gastrointest. Liver Physiol. 300, G723–728.

Bhattacharjee, A., Shukla, M., Yakubenko, V.P., Mulya, A., Kundu, S., Cathcart, M.K., 2013. IL-4 and IL-13 employ discrete signaling pathways for target gene expression in alternatively activated monocytes/macrophages. Free Radic. Biol. Med. 54, 1–16.

Borthwick, L.A., Barron, L., Hart, K.M., Vannella, K.M., Thompson, R.W., Oland, S., Cheever, A., Sciurba, J., Ramalingam, T.R., Fisher, A.J., Wynn, T.A., 2016. Macrophages are critical to the maintenance of IL-13-dependent lung inflammation and fibrosis. Mucosal Immunol. 9, 38–55.

Butler, M., Crooke, R.M., Graham, M.J., Lemonidis, K.M., Lougheed, M., Murray, S.F., Witchell, D., Steinbrecher, U., Bennett, C.F., 2000. Phosphorothioate oligodeoxynucleotides distribute similarly in class A scavenger receptor knockout and wild-type mice. J. Pharmacol. Exp. Ther. 292, 489–496.

Campbell, A.C., Dronfield, M.W., Toghill, P.J., Reeves, W.G., 1981. Neutrophil function in chronic liver disease. Clin. Exp. Immunol. 45, 81–89.

Chandriani, S., DePianto, D.J., N'Diaye, E.N., Abbas, A.R., Jackman, J., Bevers 3rd, J., Ramirez-Carrozzi, V., Pappu, R., Kauder, S.E., Toy, K., Ha, C., Modrusan, Z., Wu, L.C., Collard, H.R., Wolters, P.J., Egen, J.G., Arron, J.R., 2014. Endogenously expressed IL-13Ralpha2 attenuates IL-13-mediated responses but does not activate signaling in human lung fibroblasts. J. Immunol. 193, 111–119.

Chang, T.T., Liaw, Y.F., Wu, S.S., Schiff, E., Han, K.H., Lai, C.L., Safadi, R., Lee, S.S., Halota, W., Goodman, Z., Chi, Y.C., Zhang, H., Hindes, R., Iloeje, U., Beebe, S., Kreter, B., 2010. Long-term entecavir therapy results in the reversal of fibrosis/cirrhosis and continued histological improvement in patients with chronic hepatitis B. Hepatology 52, 886–893.

Cheever, A.W., Williams, M.E., Wynn, T.A., Finkelman, F.D., Seder, R.A., Cox, T.M., Hieny, S., Caspar, P., Sher, A., 1994. Anti-IL-4 treatment of *Schistosoma mansoni*-infected mice inhibits development of T cells and non-B, non-T cells expressing Th2 cytokines while decreasing egg-induced hepatic fibrosis. J. Immunol. 153, 753–759.

Chiaramonte, M.G., Donaldson, D.D., Cheever, A.W., Wynn, T.A., 1999. An IL-13 inhibitor blocks the development of hepatic fibrosis during a T-helper type 2-dominated inflammatory response. J. Clin. Invest. 104, 777–785.

D'Ambrosio, R., Aghemo, A., Rumi, M.G., Ronchi, G., Donato, M.F., Paradis, V., Colombo, M., Bedossa, P., 2012. A morphometric and immunohistochemical study to assess the benefit of a sustained virological response in hepatitis C virus patients with cirrhosis. Hepatology 56, 532–543.

Duffield, J.S., Lupher, M., Thannickal, V.J., Wynn, T.A., 2013. Host responses in tissue repair and fibrosis. Annu. Rev. Pathol. 8, 241–276.

Egawa, M., Mukai, K., Yoshikawa, S., Iki, M., Mukaida, N., Kawano, Y., Minegishi, Y., Karasuyama, H., 2013. Inflammatory monocytes recruited to allergic skin acquire an anti-inflammatory M2 phenotype via basophil-derived interleukin-4. Immunity 38, 570–580.

Fichtner-Feigl, S., Strober, W., Kawakami, K., Puri, R.K., Kitani, A., 2006. IL-13 signaling through the IL-13alpha2 receptor is involved in induction of TGF-beta1 production and fibrosis. Nat. Med. 12, 99–106.

Fichtner-Feigl, S., Fuss, I.J., Young, C.A., Watanabe, T., Geissler, E.K., Schlitt, H.J., Kitani, A., Strober, W., 2007. Induction of IL-13 triggers TGF-beta1-dependent tissue fibrosis in chronic 2,4,6-trinitrobenzene sulfonic acid colitis. J. Immunol. 178, 5859–5870.

Friedman, S.L., Sheppard, D., Duffield, J.S., Violette, S., 2013. Therapy for fibrotic diseases: nearing the starting line. Sci. Transl. Med. 5 (167sr161).

Gordon, S., Martinez, F.O., 2010. Alternative activation of macrophages: mechanism and functions. Immunity 32, 593–604.

Gundra, U.M., Girgis, N.M., Gonzalez, M.A., San Tang, M., Van Der Zande, H.J.P., Lin, J.D., Ouimet, M., Ma, L.J., Poles, J., Vozhilla, N., Fisher, E.A., Moore, K.J., Loke, P., 2017. Vitamin a mediates conversion of monocyte-derived macrophages into tissue-resident macrophages during alternative activation. Nat. Immunol. 18, 642–653.

Hao, H., Cohen, D.A., Jennings, C.D., Bryson, J.S., Kaplan, A.M., 2000. Bleomycin-induced pulmonary fibrosis is independent of eosinophils. J. Leukoc. Biol. 68, 515–521.

Herbert, D.R., Holscher, C., Mohrs, M., Arendse, B., Schwegmann, A., Radwanska, M., Leeto, M., Kirsch, R., Hall, P., Mossmann, H., Claussen, B., Forster, I., Brombacher, F., 2004. Alternative macrophage activation is essential for survival during schistosomiasis and downmodulates T helper 1 responses and immunopathology. Immunity 20, 623–635.

Issa, R., Zhou, X., Constandinou, C.M., Fallowfield, J., Millward-Sadler, H., Gaca, M.D., Sands, E., Suliman, I., Trim, N., Knorr, A., Arthur, M.J., Benyon, R.C., Iredale, J.P., 2004. Spontaneous recovery from micronodular cirrhosis: evidence for incomplete resolution associated with matrix cross-linking. Gastroenterology 126, 1795–1808.

Jaguin, M., Houlbert, N., Fardel, O., Lecureur, V., 2013. Polarization profiles of human M-CSF-generated macrophages and comparison of M1-markers in classically activated macrophages from GM-CSF and M-CSF origin. Cell. Immunol. 281, 51–61.

Kaplan, M.H., Whitfield, J.R., Boros, D.L., Grusby, M.J., 1998. Th2 cells are required for the *Schistosoma mansoni* egg-induced granulomatous response. J. Immunol. 160, 1850–1856.

Karlmark, K.R., Weiskirchen, R., Zimmermann, H.W., Gassler, N., Ginhoux, F., Weber, C., Merad, M., Luedde, T., Trautwein, C., Tacke, F., 2009. Hepatic recruitment of the inflammatory Gr1+ monocyte subset upon liver injury promotes hepatic fibrosis. Hepatology 50, 261–274.

Kaviratne, M., Hesse, M., Leusink, M., Cheever, A.W., Davies, S.J., McKerrow, J.H., Wakefield, L.M., Letterio, J.J., Wynn, T.A., 2004. IL-13 activates a mechanism of tissue fibrosis that is completely TGF-beta independent. J. Immunol. 173, 4020–4029.

Kurreck, J., Wyszko, E., Gillen, C., Erdmann, V.A., 2002. Design of antisense oligonucleotides stabilized by locked nucleic acids. Nucleic Acids Res. 30, 1911–1918.

Lee, R.G., Crosby, J., Baker, B.F., Graham, M.J., Crooke, R.M., 2013. Antisense technology: an emerging platform for cardiovascular disease therapeutics. J. Cardiovasc. Transl. Res. 6, 969–980.

Lin, J.X., Migone, T.S., Tsang, M., Friedmann, M., Weatherbee, J.A., Zhou, L., Yamauchi, A., Bloom, E.T., Mietz, J., John, S., et al., 1995. The role of shared receptor motifs and common Stat proteins in the generation of cytokine pleiotropy and redundancy by IL-2, IL-4, IL-7, IL-13, and IL-15. Immunity 2, 331–339.

Madsen, D.H., Leonard, D., Masedunskas, A., Moyer, A., Jurgensen, H.J., Peters, D.E., Amornphimoltham, P., Selvaraj, A., Yamada, S.S., Brenner, D.A., Burgdorf, S., Engelholm, L.H., Behrendt, N., Holmbeck, K., Weigert, R., Bugge, T.H., 2013. M2-like macrophages are responsible for collagen degradation through a mannose receptor-mediated pathway. J. Cell Biol. 202, 951–966.

Marcellin, P., Gane, E., Buti, M., Afdhal, N., Sievert, W., Jacobson, I.M., Washington, M.K., Germanidis, G., Flaherty, J.F., Schall, R.A., Bornstein, J.D., Kitrinos, K.M., Subramanian, G.M., McHutchison, J.G., Heathcote, E.J., 2013. Regression of cirrhosis during treatment with tenofovir disoproxil fumarate for chronic hepatitis B: a 5-year open-label follow-up study. Lancet 381, 468–475.

Marra, F., DeFranco, R., Grappone, C., Milani, S., Pastacaldi, S., Pinzani, M., Romanelli, R.G., Laffi, G., Gentilini, P., 1998. Increased expression of monocyte chemotactic protein-1 during active hepatic fibrogenesis: correlation with monocyte infiltration. Am. J. Pathol. 152, 423–430.

McHedlidze, T., Waldner, M., Zopf, S., Walker, J., Rankin, A.L., Schuchmann, M., Voehringer, D., McKenzie, A.N., Neurath, M.F., Pflanz, S., Wirtz, S., 2013. Interleukin-33-dependent innate lymphoid cells mediate hepatic fibrosis. Immunity 39, 357–371.

McKenzie, G.J., Fallon, P.G., Emson, C.L., Grencis, R.K., McKenzie, A.N., 1999. Simultaneous disruption of interleukin (IL)-4 and IL-13 defines individual roles in T helper cell type 2-mediated responses. J. Exp. Med. 189, 1565–1572.

Mehal, W.Z., Schuppan, D., 2015. Antifibrotic therapies in the liver. Semin. Liver Dis. 35, 184–198.

Minutti, C.M., Jackson-Jones, L.H., Garcia-Fojeda, B., Knipper, J.A., Sutherland, T.E., Logan, N., Ringqvist, E., Guillamat-Prats, R., Ferenbach, D.A., Artigas, A., Stamme, C., Chroneos, Z.C., Zaiss, D.M., Casals, C., Allen, J.E., 2017. Local amplifiers of IL-4Ralpha-mediated macrophage activation promote repair in lung and liver. Science 356, 1076–1080.

Mohrs, M., Ledermann, B., Kohler, G., Dorfmuller, A., Gessner, A., Brombacher, F., 1999. Differences between IL-4- and IL-4 receptor alpha-deficient mice in chronic leishmaniasis reveal a protective role for IL-13 receptor signaling. J. Immunol. 162, 7302–7308.

Murray, P.J., Allen, J.E., Biswas, S.K., Fisher, E.A., Gilroy, D.W., Goerdt, S., Gordon, S., Hamilton, J.A., Ivashkiv, L.B., Lawrence, T., Locati, M., Mantovani, A., Martinez, F.O., Mege, J.L., Mosser, D.M., Natoli, G., Saeij, J.P., Schultze, J.L., Shirey, K.A., Sica, A., Suttles, J., Udalova, I., van Ginderachter, J.A., Vogel, S.N., Wynn, T.A., 2014. Macrophage activation and polarization: nomenclature and experimental guidelines. Immunity 41, 14–20.

Nilsson, G., Nilsson, K., 1995. Effects of interleukin (IL)-13 on immediate-early response gene expression, phenotype and differentiation of human mast cells. Comparison with IL-4. Eur. J. Immunol. 25, 870–873.

Ochi, H., De Jesus, N.H., Hsieh, F.H., Austen, K.F., Boyce, J.A., 2000. IL-4 and -5 prime human mast cells for different profiles of IgE-dependent cytokine production. Proc. Natl. Acad. Sci. U. S. A. 97, 10509–10513.

Pellicoro, A., Aucott, R.L., Ramachandran, P., Robson, A.J., Fallowfield, J.A., Snowdon, V.K., Hartland, S.N., Vernon, M., Duffield, J.S., Benyon, R.C., Forbes, S.J., Iredale, J.P., 2012. Elastin accumulation is regulated at the level of degradation by macrophage metalloelastase (MMP-12) during experimental liver fibrosis. Hepatology 55, 1965–1975.

Pesce, J.T., Ramalingam, T.R., Mentink-Kane, M.M., Wilson, M.S., El Kasmi, K.C., Smith, A. M., Thompson, R.W., Cheever, A.W., Murray, P.J., Wynn, T.A., 2009. Arginase-1-expressing macrophages suppress Th2 cytokine-driven inflammation and fibrosis. PLoS Pathog. 5, e1000371.

Popov, Y., Patsenker, E., Fickert, P., Trauner, M., Schuppan, D., 2005. Mdr2 (Abcb4)−/− mice spontaneously develop severe biliary fibrosis via massive dysregulation of pro- and antifibrogenic genes. J. Hepatol. 43, 1045–1054.

Popov, Y., Sverdlov, D.Y., Sharma, A.K., Bhaskar, K.R., Li, S., Freitag, T.L., Lee, J., Dieterich, W., Melino, G., Schuppan, D., 2011. Tissue transglutaminase does not affect fibrotic matrix stability or regression of liver fibrosis in mice. Gastroenterology 140, 1642–1652.

Ramachandran, P., Pellicoro, A., Vernon, M.A., Boulter, L., Aucott, R.L., Ali, A., Hartland, S.N., Snowdon, V.K., Cappon, A., Gordon-Walker, T.T., Williams, M.J., Dunbar, D.R., Manning, J.R., van Rooijen, N., Fallowfield, J.A., Forbes, S.J., Iredale, J.P., 2012. Differential Ly-6C expression identifies the recruited macrophage phenotype, which orchestrates the regression of murine liver fibrosis. Proc. Natl. Acad. Sci. U. S. A. 109, E3186–3195.

Richter, A., Puddicombe, S.M., Lordan, J.L., Bucchieri, F., Wilson, S.J., Djukanovic, R., Dent, G., Holgate, S.T., Davies, D.E., 2001. The contribution of interleukin (IL)-4 and IL-13 to the epithelial-mesenchymal trophic unit in asthma. Am. J. Respir. Cell Mol. Biol. 25, 385–391.

Schuppan, D., Afdhal, N.H., 2008. Liver cirrhosis. Lancet 371, 838–851.

Schuppan, D., Kim, Y.O., 2013. Evolving therapies for liver fibrosis. J. Clin. Invest. 123, 1887–1901.

Seth, P.P., Siwkowski, A., Allerson, C.R., Vasquez, G., Lee, S., Prakash, T.P., Kinberger, G., Migawa, M.T., Gaus, H., Bhat, B., Swayze, E.E., 2008. Design, synthesis and evaluation of constrained methoxyethyl (cMOE) and constrained ethyl (cEt) nucleoside analogs. Nucleic Acids Symp. Ser. 553–554.

Sher, A., Coffman, R.L., Hieny, S., Scott, P., Cheever, A.W., 1990. Interleukin 5 is required for the blood and tissue eosinophilia but not granuloma formation induced by infection with *Schistosoma mansoni*. Proc. Natl. Acad. Sci. U. S. A. 87, 61–65.

Shimizu, Y., Murata, H., Kashii, Y., Hirano, K., Kunitani, H., Higuchi, K., Watanabe, A., 2001. CC-chemokine receptor 6 and its ligand macrophage inflammatory protein 3alpha might be involved in the amplification of local necroinflammatory response in the liver. Hepatology 34, 311–319.

Sica, A., Invernizzi, P., Mantovani, A., 2014. Macrophage plasticity and polarization in liver homeostasis and pathology. Hepatology 59, 2034–2042.

Stein, M., Keshav, S., Harris, N., Gordon, S., 1992. Interleukin 4 potently enhances murine macrophage mannose receptor activity: a marker of alternative immunologic macrophage activation. J. Exp. Med. 176, 287–292.

Tacke, F., Zimmermann, H.W., 2014. Macrophage heterogeneity in liver injury and fibrosis. J. Hepatol. 60, 1090–1096.

Tomkinson, A., Duez, C., Cieslewicz, G., Pratt, J.C., Joetham, A., Shanafelt, M.C., Gundel, R., Gelfand, E.W., 2001. A murine IL-4 receptor antagonist that inhibits IL-4- and IL-13-induced responses prevents antigen-induced airway eosinophilia and airway hyperresponsiveness. J. Immunol. 166, 5792–5800.

Trautwein, C., Friedman, S.L., Schuppan, D., Pinzani, M., 2015. Hepatic fibrosis: concept to treatment. J. Hepatol. 62, S15–24.

Vannella, K.M., Barron, L., Borthwick, L.A., Kindrachuk, K.N., Narasimhan, P.B., Hart, K.M., Thompson, R.W., White, S., Cheever, A.W., Ramalingam, T.R., Wynn, T.A., 2014. Incomplete deletion of IL-4Ralpha by LysM(Cre) reveals distinct subsets of M2 macrophages controlling inflammation and fibrosis in chronic schistosomiasis. PLoS Pathog. 10, e1004372.

Wang, X., Hausding, M., Weng, S.Y., Kim, Y.O., Steven, S., Klein, T., Daiber, A., Schuppan, D., 2018. Gliptins suppress inflammatory macrophage activation to mitigate inflammation, fibrosis, oxidative stress, and vascular dysfunction in models of nonalcoholic steatohepatitis and liver fibrosis. Antioxid. Redox Signal. 28, 87–109.

Wanless, I.R., Nakashima, E., Sherman, M., 2000. Regression of human cirrhosis. Morphologic features and the genesis of incomplete septal cirrhosis. Arch. Pathol. Lab. Med. 124, 1599–1607.